2114 *Chem. Mater.* **2010,** *22,* 2114–2119
DOI:10.1021/cm903651e

CHEMISTRY OF MATERIALS
Article

Hydrogen-Bonded Dicubane Co^{II}_7 Single-Molecule-Magnet Coordinated by in Situ Solvothermally Generated 1,2-Bis(8-hydroxyquinolin-2-yl)-ethane-1,2-diol Arranged in a Trefoil

Qing Chen,[†] Ming-Hua Zeng,*[,†] Yan-Ling Zhou,[†] Hua-Hong Zou,[†] and Mohamedally Kurmoo*[,‡]

[†]*Key Laboratory for the Chemistry and Molecular Engineering of Medicinal Resources (Ministry of Education), School of Chemistry & Chemical Engineering of Guangxi Normal University, Guilin 541004, P.R. China, and* [‡]*Laboratoire de Chimie de Coordination Organique, CNRS-UMR7140, Université de Strasbourg, 4 rue Blaise Pascal, 67000 Strasbourg Cedex, France*

Received December 3, 2009. Revised Manuscript Received January 21, 2010

A novel single vertex-shared dicubane-based cobalt(II) compound, $[Co^{II}_7(bhqe)_3(OH)_2(H_2O)_6]\cdot 2C_2H_5OH\cdot H_2O$ (**1**), was obtained through the solvothermal generation of 1,2-bis(8-hydroxyquinolin-2-yl)ethane-1,2-diol, H_4bhqe, from 2-(hydroxymethyl)quinolin-8-ol, H_2hmq, by in situ C−C coupling reaction in ethanol containing $Co(NO_3)_2\cdot 6H_2O$ and triethylamine. The crystal structure consists of dicubane Co_7 cores with six ligands wrapped around it in a trefoil through strong intramolecular $\pi-\pi$ interactions and features an unusual one-dimensional hydrogen-bonded ($OH_{water}\cdots O_{bhqe}$) supramolecular organization (along the *c*-axis). The key factor of the cluster is that every pair of cobalt atoms are bridged by a single oxygen atoms making an average angle of approximately 95° and is expected theoretically and experimentally to generate ferromagnetic coupling. The temperature dependence magnetization exhibits a blocking temperature at approximately 3 K which is confirmed by observation of large frequency dependence of the ac-susceptibilities in zero dc-field, and detailed analysis of the dynamics properties allows an unambiguous demonstration of the single-molecule magnet (SMM) behavior in **1**, though some interesting complexities in the slow magnetization relaxation processes may be influenced by the crystal system, the large anisotropy of cobalt(II) and the supramolecular interactions.

Introduction

In recent years we have witnessed a considerable expansion in the field of magnetism from molecular units[1,2] and metal−organic extended networks.[2] While all the conventional known magnetic ground states, which exist for metals, alloys, and oxides, still dominate the field, metal−organic systems have provided a new area of physics involving magnetism of small clusters and chains with unconventional behaviors.[2a,3] Following the first major discovery, that is, of single-molecule-magnetism (SMM), through the observation of quantum tunneling in the magnetization of $[Mn_{12}O_{12}(OOCCH_3)_{16}(OH_2)_4]$ and the slow relaxation process by the frequency dependence of its ac-susceptibilities, much research has been devoted to the development of related materials as they are thought to be potential for information storage.[1] A key result for the observation of SMM in these compounds is the negative single-ion anisotropy of the Mn^{III} while the segregation of the clusters in the solids and the structural anisotropy are also important but not strict requirements.[1a−c] As such the field has developed much more rapidly for compounds containing manganese than for other first row transition metals.[1,2] Presently, examples are known with a wide variety of homometallic systems of the d- and f-series and also heterometallic systems.[1−3] Among the homometallic

*Corresponding authors. E-mail: zmh@mailbox.gxnu.edu.cn; kurmoo@chimie.u-strasbg.fr.

(1) (a) Gatteschi, D.; Sessoli, R.; Villain, J. *Molecular Nanomagnets*; Oxford University Press: Oxford, 2006. (b) Aromí, G.; Brechin, E. K. *Struct. Bonding (Berlin)* **2006**, *122*, 1–69. (c) Gatteschi, D.; Sessoli, R. *Angew. Chem., Int. Ed.* **2003**, *42*, 268–297. (d) Stamatatos, T. C.; Christou, G. *Inorg. Chem.* **2009**, *48*, 3308–3322. (e) Rinehart, J. D.; Harris, T. D.; Kozimor, S. A.; Bartlett, B. M.; Long, J. R. *Inorg. Chem.* **2009**, *48*, 3382–3395.

(2) (a) Bogani, L.; Vindigni, A.; Sessoli, R.; Gatteschi, D. *J. Mater. Chem.* **2008**, *18*, 4750–4758. (b) Kurmoo, M. *Chem. Soc. Rev.* **2009**, *38*, 1353–1379. (c) Wang, X.-Y.; Wang, Z.-M.; Gao, S. *Chem. Commun.* **2008**, 281–291. (d) Zeng, Y.-F.; Hu, X.; Liu, F.-C.; Bu, X.-H. *Chem. Soc. Rev.* **2009**, *38*, 469–480. (e) Pardo, E.; Ruiz-García, R.; Cano, J.; Ottenwaelder, X.; Lescouëzec, R.; Journaux, Y.; Lloret, F.; Julve, M. *Dalton Trans.* **2008**, 2780–2805. (f) Andruh, M.; Costes, J.-P.; Diaz, C.; Gao, S. *Inorg. Chem.* **2009**, *48*, 3342–3359. (g) Bleuzen, A.; Marvaud, V.; Mathoniere, C.; Sieklucka, B.; Verdaguer, M. *Inorg. Chem.* **2009**, *48*, 3453–3466.

(3) (a) Rinehart, J. D.; Long, J. R. *J. Am. Chem. Soc.* **2009**, *131*, 12558–12559. (b) Hussain, B.; Savard, D.; Burchell, T. J.; Wernsdorfer, W.; Murugesu, M. *Chem. Commun.* **2009**, 1100–1102. (c) Yoshihara, D.; Karasawa, S.; Koga, N. *J. Am. Chem. Soc.* **2008**, *130*, 10460–10461. (d) Mereacre, V.; Ako, A. M.; Clérac, R.; Wernsdorfer, W.; Hewitt, I. J.; Anson, C. E.; Powell, A. K. *Chem.—Eur. J.* **2008**, *14*, 3577–3584. (e) Palii, A. V.; Reu, O. S.; Ostrovsky, S. M.; Klokishner, S. I.; Tsukerblat, B. S.; Sun, Z.-M.; Mao, J.-G.; Prosvirin, A. V.; Zhao, H.-H.; Dunbar, K. R. *J. Am. Chem. Soc.* **2008**, *130*, 14729–14738. (f) Yang, C.-I.; Wernsdorfer, W.; Lee, G.-H.; Tsai, H.-L. *J. Am. Chem. Soc.* **2007**, *129*, 456–457. (g) Milios, C. J.; Vinslava, A.; Wood, P. A.; Parsons, S.; Wernsdorfer, W.; Christou, G.; Perlepes, S. P.; Brechin, E. K. *J. Am. Chem. Soc.* **2007**, *129*, 8–9.

 Published on Web 02/02/2010

clusters of the first row transition elements, there are very few cobalt(II) compounds which are known to display SMMs behavior,[4−6] though the second major discovery in this field, that is, of single-chain-magnetism (SCM),[2a,7] was that of a cobalt(II)−organic radical chain system, $[Co^{II}(hfac)_2(NITPhOMe)]$ (hfac = hexafluoroacetylacetonate, NITPhOMe = 4′-methoxy-phenyl-4,4,5,5-tetramethylimidazoline-1-oxyl-3-oxide).[8] Although there is a vague report of SMMs for a linear trimeric cluster, the smallest well-characterized SMM clusters are primarily those containing cubane, Co_4O_4, and a couple with planar geometry.[4−6] Interestingly, most of the Co_4O_4 clusters contained citrate as the coordinating ligand.[4] We believe the observation of SMMs in these clusters is due to the ferromagnetic coupling between the nearest cobalt atoms as a result of the low Co−O−Co angles (<96°) as expected within the Goodenough−Kanamori rule, in which orthogonal hard-axis alignments of four single ion spins ($D_{ion} > 0$) may result in the negative D_{mol} value for the clusters,[5,9] although from a single-ion anisotropy point of view cobalt(II) clusters are not expected to show SMM behavior.

From the point of view of organic ligand design, it is desirable to synthesize bulky ligands that have the coordinating atoms pointing on one side of the molecule, this favoring magnetic isolation of the clusters.[1] Such an approach has been especially successfully in creating a SMM consisting of a cube-based Co_{12} supercluster by using the bulky ligand, (1*H*-benzimidazol-2-yl)-methanol (hbm).[5] As a continuation of this work on 3d transition-metal clusters,[10] we introduce here an analogous anion of 2-(hydroxymethyl)-quinolin-8-ol (H_2hmq) to serve as a pioneer ligand, and report the first example of a SMM of cobalt(II) having two fused cubanes with one common cobalt atom, $[Co^{II}_7(bhqe)_3(OH)_2(H_2O)_6]\cdot 2C_2H_5OH\cdot H_2O$ (**1**), which was obtained by the accidental in situ generation of the ligand in the solvothermal reaction. The cluster has been characterized by single-crystal structure determination and extensive magnetization measurements, using both ac and dc modes, as a function of magnetic field, temperature, and frequency.

Table 1. Crystallographic Data[a]

	1
formula	$Co_7C_{64}H_{64}O_{23}N_6$
formula weight	1697.75
crystal size (mm^3)	0.28 × 0.28 × 0.12
crystal system	trigonal
space group	$P\bar{3}c1$
T (K)	293
a (Å)	13.5006(1)
c (Å)	19.704(4)
V (Å^3)	3110.2(7)
Z	2
D_c (g cm^{-3})	1.766
μ (mm^{-1})	1.812
reflns collected	18124
unique reflns	2058
R_{int}	0.064
R_1 [$I > 2\sigma(I)$]	0.0435
wR_2 (all data)	0.1169
GOF	1.068
$\Delta\rho_{min/max}$ (e/Å^3)	−0.34/0.45

[a] $R_1 = \sum||F_o| - |F_c||/\sum|F_o|$, $wR_2 = [\sum w(|F_o| - |F_c|)^2/\sum w|F_o|^2]^{1/2}$.

Experimental Section

Materials and Physical Measurements. All reagents were commercially available and used without further purification. Infrared spectra were recorded by transmission through KBr pellets containing about 1% of the compound using a PE Spectrum One FT-IR spectrometer in the 400−4000 cm^{-1} region. Elemental analyses (C, H, N) were performed on a PE Series 2400-CHNS analyzer. Thermal analyses (DT-TGA) were performed at a rate of 10 °C/min under N_2 using a Pyris Diamond TG/DTA thermogravimetric/differential thermal analyzer. Powder X-ray diffraction (PXRD) data were recorded on a Rigaku D/M-2200T automated diffractometer. AC and DC magnetization measurements of **1** were performed on polycrystalline samples using a Quantum Design MPMS-XL5 SQUID. Data were corrected for the diamagnetic contribution calculated from Pascal constants and the sample container.

X-ray Crystallography. Diffraction data were collected on a Bruker Smart Apex CCD diffractometer with graphite monochromated Mo Kα radiation ($\lambda = 0.71073$ Å). All intensity data were corrected for Lorentz and polarization effects, and empirical absorption corrections based on equivalent reflections were applied (SADABS). The structure was solved by direct methods and refined by the full-matrix least-squares method on F^2 using the SHELXTL program package.[11] All non-hydrogen atoms were refined with anisotropic displacement parameters. The hydrogen atoms were generated geometrically. Crystal data as well as details of data collection and refinements are summarized in Table 1. Selected bond distances and bond angles are listed in Table 2. The supplementary crystallographic data for this paper can be found in the Supporting Information or can be obtained free of charge from the Cambridge Crystallographic Data Centre via http://www.ccdc.cam.ac.uk/data_request/cif (CCDC-694860).

Results and Discussion

Synthesis. An important reaction leading to the formation of these crystals is the in situ solvothermal dimerization

(4) (a) Murrie, M.; Teat, S. J.; Stœkli-Evans, H.; Güdel, H. U. *Angew. Chem., Int. Ed.* **2003**, *42*, 4653–4656. (b) Moubaraki, B.; Murray, K. S.; Hudson, T. A.; Robson, R. *Eur. J. Inorg. Chem.* **2008**, 4525–4529. (c) Galloway, K. W.; Whyte, A. M.; Wernsdorfer, W.; Sanchez-Benitez, J.; Kamenev, K. V.; Parkin, A.; Peacock, R. D.; Murrie, M. *Inorg. Chem.* **2008**, *47*, 7438–7442.
(5) Zeng, M.-H.; Yao, M.-X.; Liang, H.; Zhang, W.-X.; Chen, X.-M. *Angew. Chem., Int. Ed.* **2007**, *46*, 1832–1835.
(6) (a) Wu, D.-Y.; Guo, D.; Song, Y.; Huang, W.; Duan, C.-Y.; Meng, Q.-J.; Sato, O. *Inorg. Chem.* **2009**, *48*, 854–860. (b) Yang, E.-C.; Hendrickson, D. N.; Wernsdorfer, W.; Nakano, M.; Zakharov, L. N.; Sommer, R. D.; Rheingold, A. L.; Ledezma-Gairaud, M.; Christou, G. *J. Appl. Phys.* **2002**, *91*, 7382–7384. (c) King, P.; Clérac, R.; Wernsdorfer, W.; Anson, C. E.; Powell, A. K. *Dalton Trans.* **2004**, 2670–2676.
(7) Coulon, C.; Miyasaka, H.; Clérac, R. *Struct. Bonding (Berlin)* **2006**, *122*, 163–206.
(8) Caneschi, A.; Gatteschi, D.; Lalioti, N.; Sangregorio, C.; Sessoli, R.; Venturi, G.; Vindigni, A.; Rettori, A.; Pini, M. G.; Novak, M. A. *Angew. Chem., Int. Ed.* **2001**, *40*, 1760–1763.
(9) (a) Oshio, H.; Nakano, M. *Chem.—Eur. J.* **2005**, *11*, 5178–5185. (b) Goodenough, J. B. *Magnetism and the Chemical Bond*; Interscience: New York, 1963.
(10) (a) Zhou, Y.-L.; Meng, F.-Y.; Zhang, J.; Zeng, M.-H.; Liang, H. *Cryst. Growth Des.* **2009**, *9*, 1402–1410. (b) Li, B.-W.; Zhou, Y.-L.; Chen, Q.; Zeng, M.-H. *Polyhedron* **2010**, *29*, 148–153.
(11) *SHELXTL 6.10*; Bruker Analytical Instrumentation: Madison, WI, U.S.A., 2000.

Table 2. Summary of the Geometrical Data of Selected Bond Lengths and Exchange Bridges for 1 (in Å and deg)[a]

Co1−O1	2.075(2)	Co2−O1−Co2B	96.18(1)
Co2−O1	2.181(3)	Co2−O3−Co2B	99.86(1)
Co2−O1A	2.088(3)	Co1−O1−Co2B	94.23(1)
Co2−O2	2.025(3)	Co1···Co2 (intracluster)	3.0502(7)
Co2−O3	2.076(2)	Co2···Co2B (intracluster)	3.1777(1)
Co2−O1W	2.215(4)	Co1···Co1C (intercluster)	9.852(2)
Co2−N1	2.070(4)	Co2···Co2D (intercluster)	5.3057(1)
Co1−O1−Co2	91.52(1)	Co2···Co2C (intercluster)	6.1845(1)

[a] Symmetry codes: (A) $-y, x-y, z$, (B) $-x+y, -x, z$, (C) $-x, -y, -z$, (D) $x-y, x, -z$.

Scheme 1. Proposed Reaction Leading to $bhqe^{4-}$ and Its Coordination Mode in 1

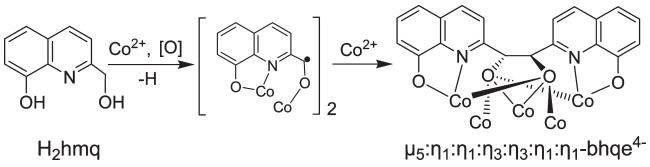

of the starting H_2hmq ligand, in the presence of the other reagents in ethanol resulting in the generation of H_4bhqe. So far, several examples of solvothermal C−C bond formation have been reported,[12] the reactions may involve radical processes, and the oxidants may come from different sources to catalyze the progress of the reaction. However, there was no oxidant mentioned in some cases. Dehydrogenative coupling of C−C single bonds are rarely reported in contrast to the well-documented dehydrogenative coupling of N-heterocycle in their metal complexes.[12,13] Herein (Scheme 1), the formation of Co^{III} by oxygen under alkaline condition during the process of the pretreatments of Co^{II} may act as the oxidant. The dehydrogenative C−C coupling reactions involve the metal-mediated procedures of the nucleophilic attack of hydroxide and boost the activation of the neighboring methylene groups, and then there is an opportunity to generate radicals on the methylene groups.[13] It suggests that the coordination behaviors of the metal ion is critical in activating the organic ligand while no oxidative ability is required in this step.[14] The complicated synthesis provides an unexpected structure for compound **1** from that of a simpler one expected with the precursor ligand, but the production of crystals large enough for single crystal magnetization measurements was difficult (Figure 1).

Crystal Structure. The crystal structure of **1** is quite unique with the key feature being the inorganic Co−O core consisting of a cluster of seven cobalt atoms disposed at the corners of two cubes with one shared at one vertex. The cobalt atoms are octahedrally coordinated via the oxygen and nitrogen atoms of the water and the organic ligand; the latter being arranged as a trefoil creating a shield around the inorganic moiety (Figure 2). These metal-organic clusters are then arranged in a hexagonal close packed fashion in layers parallel to each other in the *ab*-plane (Figure 3). The unit cell contains two such layers where the two geometrical enantiomers are segregated and stacked in an ABAB mode. The center-to-center distance between clusters is 13.5 Å within the layer and that between layers is 9.85 Å (Figure 4). This particular Co−O heptanuclear core has been observed before in the 3D-coordination polymer, $Co_7(\mu_3-OH)_8(ox)_3(pip)_3$, where they are bridged by piperazine and oxalate;[15]

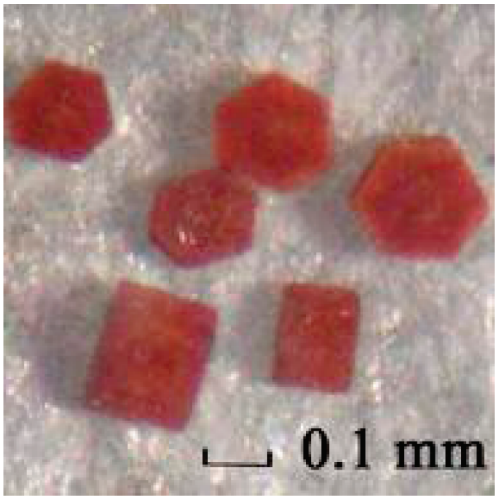

Figure 1. Photo of some single crystals of **1** showing the morphology and size.

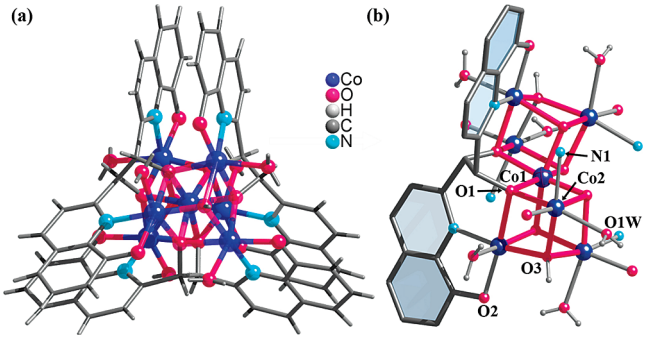

Figure 2. (a) Heptanuclear unit of **1**, guest molecules are omitted for clarity; (b) the Co_7 core with selected atom-labeling scheme. Some hydrogen atoms are omitted for clarity.

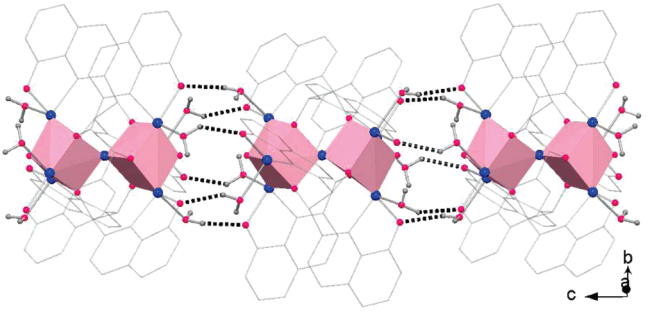

Figure 3. 1D 6-fold hydrogen-bonding chain along the *c* axis.

(12) (a) Liu, C.-M.; Gao, S.; Kou, H.-Z. *Chem. Commun.* **2001**, 1670–1671. (b) Hu, S.; Chen, J.-C.; Tong, M.-L.; Wang, B.; Yan, Y.-X.; Batten, S. R. *Angew. Chem., Int. Ed.* **2005**, *44*, 5471–5475.
(13) Chen, X.-M.; Tong, M.-L. *Acc. Chem. Res.* **2007**, *40*, 162–170.
(14) Zheng, N.-F; Bu, X.-H; Feng, P.-Y. *J. Am. Chem. Soc.* **2002**, *124*, 9688–9689.
(15) Chiang, R.-K.; Huang, C.-C.; Wur, C.-S. *Inorg. Chem.* **2001**, *40*, 3237–3239.

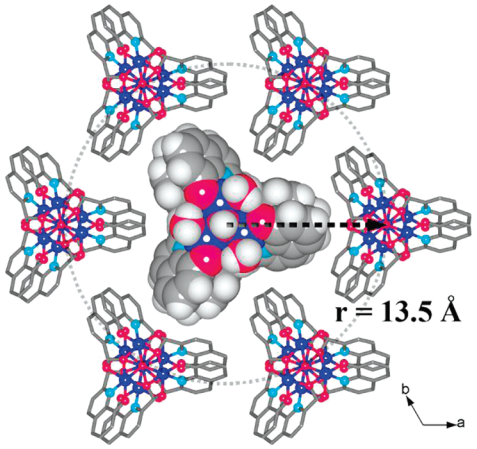

Figure 4. Packing diagram of **1** in the *ab*-plane.

however, the present structure reveals the first example of a discrete heteronuclear dicubane motif.[16]

In detail, the core contains seven Co^{II} ions, two μ_3-bridging hydroxide ions, and six alkoxo oxygen atoms of three μ_5:η_1:η_1:η_3:η_3:η_1:η_1-bhqe^{4-} anions (Scheme 1). Co1 is coordinated by six μ_3-alkoxo oxygen atoms from three bhqe^{4-} anion. The six symmetry equivalent Co2 atoms are arranged in a staggered fashion, three up and three down along the *c*-axis, sandwiching the Co1. Each Co2 adopts a distorted $CoNO_5$ octahedron formed by two bhqe^{4-}, μ_3-alkoxo oxygen atoms, two O,N-chelating sites, one μ_3-hydroxide ion, and a terminal H_2O molecule. The cuboidal core is distorted, with distances of 3.05 Å for Co1···Co2, 3.178 Å for Co2···Co2, and the Co−O−Co angles in the range of 95 ± 4°; these distances and angles are expected to favor ferromagnetic exchange.[5,9,10] However, if the exchange between a pair of cobalt atoms is antiferromagnetic, a highly magnetically frustrated cluster is anticipated similar to the case of pyrochlore spin-ice systems due to the presence the tetrahedral arrangement of moments.[17] Each cluster is hydrogen-bonded, through the oxygen atoms of the chelating bhqe^{4-} groups and the axial coordinated water molecules, to its two neighbors along the *c*-axis. This leads to the formation of 1D chains with a short O1W−H1W···O2 bond (2.715(4) Å) and Co···Co separation of approximately 5.3 Å (Figure 3). Although a portion of disorder C_2H_5OH and H_2O molecules were found in the crystal lattice, each Co_7 unit is well isolated in the *ab*-plane by the bulky bhqe^{4-} ligand. There is no significant interaction between the adjacent hydrogen-bonded chains (Figure 4). This special intermolecular interaction and correlation may be important in understanding the magnetic behavior of this molecule.[18] The trefoil produced by the ligand around the cobalt core is

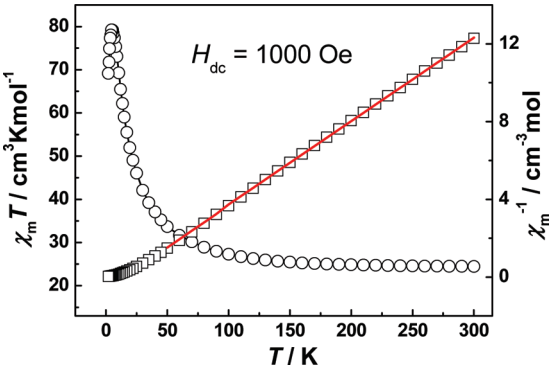

Figure 5. Temperature dependence of $\chi_m T$ and plots of χ_m^{-1} and the fit of Curie−Weiss law (solid curve) for 100−300 K of **1**.

generated by strong $\pi-\pi$ interactions between the quinoid rings where short distances of 3.29 Å (C···N), 3.44 Å (N···N), and 3.28 Å (C···C) are observed.

Magnetic Properties. Several different magnetization measurements in dc and ac modes as a function of temperature, field, and frequency were performed to characterize the compound. As the crystals were not large enough to perform measurements on a single one, we crushed the crystals into a powder to obtain good averaging of the properties. Furthermore, the crystallites were fixed to prevent torque in high fields. The dc-magnetic susceptibility data of **1** were collected on cooling in an applied field of 1000 Oe. The product of $\chi_m T$, proportional to the effective moment, increases steadily from 24.43 cm^3 K mol^{-1} at 300 K to 79.24 cm^3 K mol^{-1} at 4.5 K, and then decreases to slightly to 69.16 cm^3 mol^{-1} K at 2.0 K (Figure 5). The continuous rise on cooling suggests ferromagnetic coupling between nearest neighbor cobalt atoms, and a Curie−Weiss fit to the data shows temperature range dependence which is often the case for cobalt due to the depopulation of the upper Kramers' doublets as a consequence of spin−orbit coupling.[5] The Curie constant is 23.4(3) cm^3 mol^{-1} K, and the Weiss temperature is +12 ± 3 K (Figure 5 and Supporting Information Figure S3). The effective moment per cobalt is 5.18 cm^3 mol^{-1} K, which is on the higher end of the observed limits. The slight decrease at low temperature suggests that the moments are saturated.

The field dependence of the magnetization at 2 K increases rapidly and almost linearly in fields less than 4 kOe, then increases slowly with increasing field strength to 16.58 μ_B at 50 kOe (Figure 6). The saturation magnetization at 50 kOe approximates to 2.37 μ_B per cobalt which is close to the expected value gS for $g = 4.3$ and $S = 1/2$. Therefore, it is reasonable to conclude that the moments of all the cobalt atoms are aligned parallel,[2b,19] that is, a ferromagnet if there is a long-range magnetic ordering, otherwise a very anisotropic high spin molecule ($S = 7/2$). Interestingly, no magnetic hysteretic behavior was observed at 2 K.[5]

To further characterize the magnetic ground state, we performed a series of ac-susceptibilities measurements at

(16) Fujita, M.; Powell, A.; Creutz, C. *From the Molecular to the Nanoscale: Synthesis, Structure, and Properties*; Elsevier: Oxford, 2004; Vol. 7.
(17) Bramwell, S. T.; Gingras, M. J. P. *Science* **2001**, *294*, 1495–1501.
(18) (a) Miyasaka, H.; Yamashita, M. *Dalton Trans.* **2007**, 399–406. (b) Lecren, L.; Wernsdorfer, W.; Li, Y.-G.; Vindigni, A.; Miyasaka, H.; Clérac, R. *J. Am. Chem. Soc.* **2007**, *129*, 5045–5051. (c) Langley, S.; Helliwell, M.; Sessoli, R.; Teat, S. J.; Winpenny, E. P. R. *Inorg. Chem.* **2008**, *47*, 497–507. (d) Zhang, Y.; Wernsdorfer, W.; Pan, F.; Wanga, Z.; Gao, S. *Chem. Commun.* **2006**, 3302.
(19) Carlin, R. L. *Magnetochemistry*; Springer: Berlin, 1986.

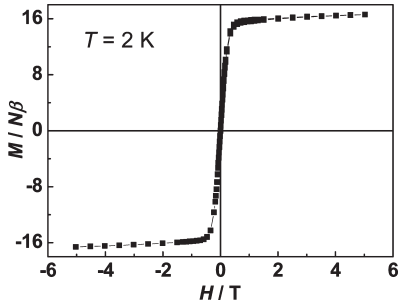

Figure 6. *M* vs *H* plot at 2 K of **1**.

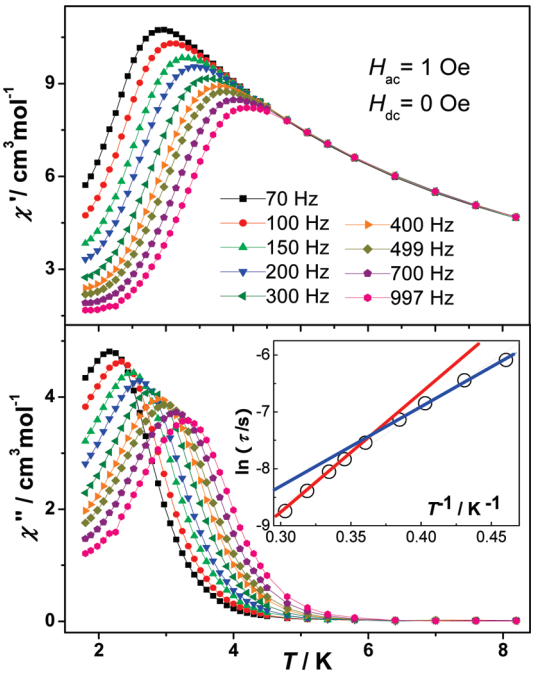

Figure 7. Temperature dependence of the in-phase χ' (top) and out-of-phase χ'' (bottom) ac-susceptibilities for **1** at different oscillating frequencies. Inset: peak temperatures of χ'' fitted to the Arrhenius law.

different frequencies using an oscillating field of 1 Oe superposed by a dc-field of zero or 600 Oe. By sweeping the temperature and measuring the ac-susceptibilities at different frequencies, the in-phase component (χ') is always finite and increases to a maximum which increases in temperature with frequency while the out-of-phase component (χ'') become nonzero below approximately 6 K and shows a maximum at a slightly lower temperature with a similar trend (Figure 7). The strong dependence on frequency is uncharacteristic of long-range ordering but common to the behavior of superparamagnets, SMM and SCM due to slow relaxation processes.[2a] To clarify the nature of the relaxation process, the peak temperature of χ' can be measured by a parameter $\Phi = (\Delta T/T)/\Delta(\log \nu) = 0.29$, which is in the range of a normal superparamagnet and precludes the possibility of a spin glass.[20] An experiment performed by sweeping the frequency of the oscillating ac-field at fixed temperature shows an Argand diagram (Cole−Cole plot, Figure 8) for temperatures

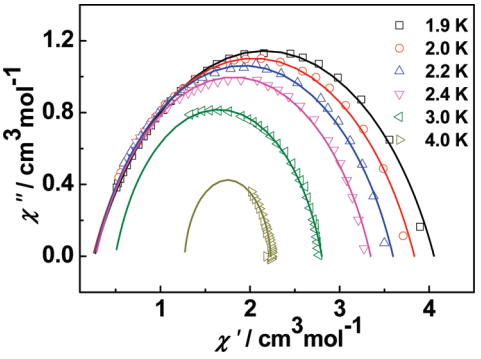

Figure 8. Cole−Cole plots between 1.9 and 4 K; solid lines represent the fit to a generalized Debye model.

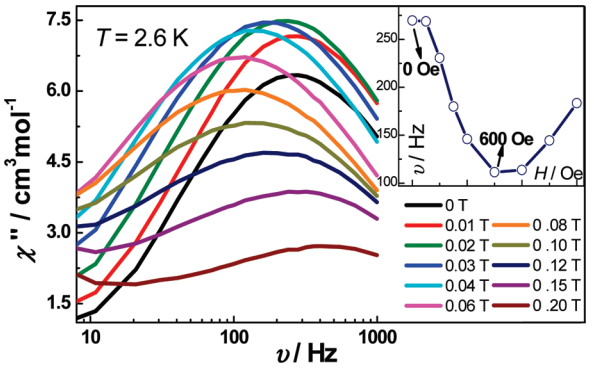

Figure 9. Frequency dependence of χ'' in different bias dc-fields at 2.6 K. Inset: deduced from the χ'' vs ν plot.

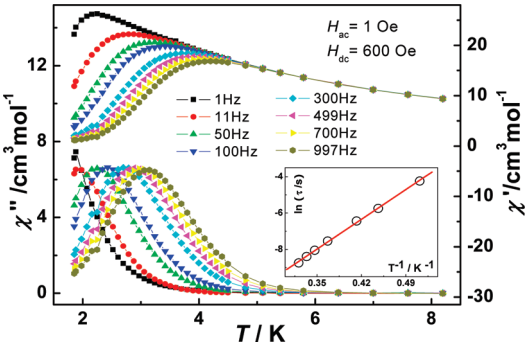

Figure 10. In-phase χ' and out-of-phase χ'' components of the ac-susceptibilities measured in a bias dc-field of 600 Oe. Inset: Peak temperatures of χ'' fitted to the Arrhenius law.

between 1.9 and 4.0 K. The single semicircular shape suggests that a simple Debye model applies and the analyses result in a relative narrow distribution of relaxation times (α = 0.21−0.30), in agreement with those observed for Co^{II}-based SMMs.[5] However, the relaxation time of **1** deduced from these measurements presents two activated regimes which follow the Arrhenius law (Figure 7 inset), above and below 2.7 K ($1/T^* = 0.37$ K) with $\Delta_{\tau 1}/k_B = 21(4)$ K, $\tau_{01} = 2.7 \times 10^{-7}$ s, and $\Delta_{\tau 2}/k_B = 13(8)$ K, $\tau_{02} = 3.9 \times 10^{-6}$ s, respectively. The appearance

(20) ϕ=0.01 is a typical value for a spin glass. For details, see Mydosh, J. A. *Spin Glasses: An Experimental Introduction*; Taylor & Francis: London, 1993.

(21) (a) Zheng, Y.-Z.; Tong, M.-L.; Zhang, W.-X.; Chen, X.-M. *Angew. Chem., Int. Ed.* **2006**, *45*, 6310–6314. (b) Kachi-Terajima, C.; Miyasaka, H.; Saitoh, A.; Shirakawa, N.; Yamashita, M.; Clérac, R. *Inorg. Chem.* **2007**, *46*, 5861–5872.

Table 3. List of the Behaviors as Well as the Gap Energy and Relaxation Times for the Compounds Containing Co_4O_4 Units

compounds	ground state	gap energy (K)	relaxation times (s)
$[(NMe_4)_3Na\{Co_4(cit)_4[Co(H_2O)_5]_2\}]\cdot 7H_2O$ (cit = citrate)[4a]	SMM	26	8.2×10^{-9}
$[(NMe_4)_4\{Co_4(cit)_4[Co(H_2O)_5]_2\}]\cdot 6H_2O$[4a]	SMM	32	2.1×10^{-9}
$[C(NH_2)_3]_8[Co_4(cit)_4]\cdot 8H_2O$[4b]	SMM	21	8×10^{-7}
$[Co_8(cit)_4(H_2O)_{12}]\cdot 24H_2O$[4b]	SMM	20.5	10×10^{-7}
$\{KCo_3(cit)(Hcit)(H_2O)_2\cdot 8H_2O\}_8$[22]	canted AF (T_N < 2 K)		
$[Co_{12}(bm)_{12}(NO_3)(OAc)_6(EtOH)_6](NO_3)_5$ (bm = benzimidazole methanol)[5]	SMM	15	1.94×10^{-7}
$[Co_4(hmp)_4(MeOH)_4Cl_4]$[6b]	SMM		
$Co_7(\mu_3\text{-}OH)_8(ox)_3(pip)_3$[15]	AF (T_N = 26 K)		
$[Co_7(bhqe)_3(OH)_2(H_2O)_6]\cdot 2C_2H_5OH\cdot H_2O$ (this work)	SMM	21, 13	2.7×10^{-7}, 3.9×10^{-6}

of a crossover in the Arrhenius plot is similar to the observed SCMs and associated to finite-size effects and has been predicted and experimentally observed for systems with a slow relaxation of single monomer units.[2a,21]

As a result of the lack of hysteresis and any steps in the isothermal magnetization loop below the blocking temperature (T_B), which normally would have confirmed SMM behavior, we did a search for the first level crossing the spectrum by measuring the frequency dependence of the ac-susceptibilities at different bias dc-field below T_B. Apparently a variety of effects can alter the magnetization dynamics of superparamagnets, for example, applying a dc-field will alter the QTM relaxation pathway and the Zeeman effects will remove the degeneracy of the $\pm M_S$ levels.[2a,18] By plotting the value of χ'', which relates to the absorption, as a function of frequency we osberved a minimum in the peak frequency at a field of 600 Oe suggesting the location of the first level crossing (Figure 9). Consequently, we performed a temperature dependence run of the ac-susceptibilities at different frequencies in a fixed dc-field of 600 Oe. Although it is slightly perturbed from the one at zero field, similar analysis of the relaxation time gives only one period regime, $\tau_0 = 9.31 \times 10^{-8}$ s and $\Delta_\tau = 23.4$ K (Figure 10).

The parameters defining the characteristics of **1** are very similar to those defining the cobalt containing single-molecule magnets in the literature.[4−6] These are collected in Table 3. While the energy barriers to magnetization reversal are not so different, the relaxation rates span 3 orders of magnitude and are faster than the Mn^{III} containing SMMs.[1] Furthermore, there is hardly any hysteresis in the cobalt containing SMMs which has been associated with the relatively rapid relaxation rate.[4−6] Whether the faster rate in the present cluster is due to the extensive hydrogen bonding, which resulted in supramolecular chains, remains to be unraveled.[18]

Notably, the magnetic properties **1** are similar to those of the dinuclear Mn_2 compound, in which the $[Mn_2(salpn)_2(H_2O)_2]^{2+}$ units linked through twofold hydrogen bonds (O−Hwater···Oph 2.733(2) Å) forming supramolecular chains resulting in the magnetic behaviors described at the frontier of SMMs and SCMs.[18b] It is dissimilar to that of our previously reported on a well isolated cubane-based, triangular Co_{12} supercluster, which behaves as a SMMs, in spite of an Ising type ferromagnetic coupling of the large number of 12 Kramers doublets. Less conspicuous magnetization relaxation can be observed for the Co_{12} cluster above 1.8 K,[5] whereas attractive relaxation dynamics is displayed owing to the infinite hydrogen bonding in **1**. It is also different from the case of homospin helical Co^{II}-based SCM reported by Gao et al.,[23] with the strong intrachain magnetic coupling through azide bridges, which is not in the Ising limit, and large domain walls are probably relevant with the $\Delta_\xi = 80$ K, $\Delta_\tau = 94$ K; both energy gaps are larger than that of **1**. This is compared with the very recently reported linear Mn_6 SMMs,[24] through the dicarboxylate linkers (iso-phthalate and succinate) with primary SMM behavior rather than staggered magnetization of antiferromagnetic finite-sized chains of SMMs. Apparently, different kinds of weak exchange approaches resulted in distinct efficiency of magnetic interaction and correlation among clusters and played quite different roles in magnetic propagation between Mn_6 system and **1**.

Conclusion

The fortunate in situ generation of 1,2-bis(8-hydroxyquinolin-2-yl)ethane-1,2-diol from 2-(hydroxymethyl)-quinolin-8-ol by the rare C−C coupling reaction resulted in the formation of the unique cluster, where the organic ligand wrapped a vertex-shared dicubane cobalt(II) unit in a trefoil fashion. Strong intramolecular $\pi-\pi$ and intermolecular interactions serve to strengthen the packing within and between clusters in the crystal. Magnetic studies reveal clear evidence of single-molecule-magnet behavior, though some complexities in the slow magnetization relaxation processes may be influenced by the crystal system, the large anisotropy of cobalt(II), and the supramolecular interactions.

Acknowledgment. This work was supported by NSFC (No. 20871034), NSFGX (No. 00832001Z), Program for New Century Excellent Talents in University of the Ministry of Education China (NCET-07-217), Project of Ten, Hundred, Thousand Distinguished Talents in New Century of Guangxi (No. 2006201), Ying Tung Education Foundation (No. 111014), and the Université de Strasbourg and CNRS (France).

Supporting Information Available: Crystallographic data (CIF); XRD and TG measurements, plots of χ^{-1} vs T and the fit of Curie−Weiss law at some different temperatures ranges (PDF). This material is available free of charge via the Internet at http://pubs.acs.org.

(22) Xiang, S.-C.; Wu, X.-T.; Zhang, J.-J.; Fu, R.-B.; Hu, S.-M.; Zhang, X.-D. *J. Am. Chem. Soc.* **2005**, *127*, 16352–16353.

(23) Liu, T.-F.; Fu, D.; Gao, S.; Zhang, Y.-Z.; Sun, H.-L.; Su, G.; Liu, Y.-J. *J. Am. Chem. Soc.* **2003**, *125*, 13976–13977.

(24) Jones, L. F.; Prescimone, A.; Evangelisti, M.; Brechin, E. K. *Chem. Commun.* **2009**, *15*, 2023–2025.